Electronic Supplementary Material (ESI) for Journal of Materials Chemistry C.

Supporting information

Research on tin-copper bimetallic phosphide nanoparticles as anode for sodium-ion batteries

Contents:

1. Experimental

First, add Y mmol stannous chloride dihydrate $SnCl_2 \cdot 2H_2O$, X mmol copper nitrate $(CuNO_3)_2 \cdot 5H_2O$ (X+Y=10, X=1, 2, 3) to 100 ml deionized water (DIW) and 100 ml N-dimethylformamide (DMF), add 15 ml HCl, stir 5min, add 15 g 1,2-diaminopropane ($C_3H_{10}N_2$), and continue to stir 30 min. Then an appropriate amount of sodium borohydride $NaBH_4$ is added to the above solution. Stir the whole mixture continuously for 12 h. The black precipitates were collected by centrifuge, washed three times with DIW and DMF, and dried in 80℃ vacuum. SnCu-X (X = 1, 2, or 3) nanoparticles were prepared.

The 0.1 g SnCu-X (X=1, 2 or 3) and 20 mg porous carbon (PC) were added to 30 ml DMF solution, ultrasonic treatment at room temperature, and continuous stirring of 30 min. 0.2 g white phosphorus was added to the solution, and the solution was transferred to 50 ml stainless steel sealed polytetrafluoroethylene autoclave. The reaction temperature is 180 ℃ and the reaction time is 16 h. After the reaction, the high-pressure tank is cooled to room temperature, the black precipitate is centrifuged and washed for 3 times with anhydrous ethanol, benzene and distilled water. The product was dried in a vacuum oven and named Sn_4P_3/PC, SnCuP/PC-1, SnCuP/PC-2 and SnCuP/PC-3.

2. Material characterization

The X-ray powder diffraction (XRD) patterns of the as-prepared products were recorded by a Japan Rigaku D/Max-3c X-ray diffraction solutions with a Cu Kα radiation (λ= 1.5418 Å). The crystal structure, surface morphology and particle size of

the as-prepared products were examined by field emission scanning electron microscope (FESEM, Hitachi S-4800, Japan), transmission electron microscopy (TEM), high-resolution transmission electron microscope (HRTEM) on a FEI Tecnai G^2 F20 apparatus with an accelerating voltage of 200 Kv. The Raman spectra were investigated on a LABRAM-HR laser confocal micro-Raman. Spectrometer X-ray photoelectron spectroscopy (XPS) of the Samples was measured on an AXIS SUPRA (Kratos). Thermogravimetric (TGA) analysis was characterized with TGA Q500, at a heating rate of 5 °C min^{-1} in air.

3. Electrochemical measurements

The electrochemical test was performed using a CR2025 button battery assembled in a glove box filled with argon. The SnCuP/PC-X, conductive carbon black, and PVDF binder were uniformly grounded in an agate mortar at a mass ratio of 7:2:1, then N-methy l-2-pyrrolidone (NMP) was added to grind for 3 - 4 h to form a slurry. The slurry was coated on a copper foil and dried at 80 ℃ for 12 h in a vacuum oven. The coated copper foil was cut into a disc with a diameter of 12 mm, which was used as the working anode for SIBs.

The assembly of SIBs was carried out in a glove box filled with argon. The SIBs are assembled using sodium metal as the counter electrode and the reference electrode. The ethyl carbonate diethyl carbonate（EC/DMC）(1/1, vol %) of 1 M $NaClO_4$ was added with 10 % fluoroethylene carbonate（FEC）additive as electrolyte. Glass microfiber membrane (GF/D, Whatman) was used as battery separator. All coin cells were tested for electrochemical properties at different charge-discharge current

densities of 200 to 2000 mA g^{-1} in the voltage limit of 0.01-3.0 V using the battery test system (CT-3008-5V 10mA). Cyclic voltammetry (CV) measurements were performed by an electrochemical workstation (CHI600E) from 0.01-3.0 V at a scan rate of 0.2-1 mV s^{-1}. The electrochemical impedance spectroscopy was measured at an amplitude of 5.0 mV in the frequency range from 100 kHz to 0.1 Hz on the same electrochemical workstation.

4.Supplementary figure

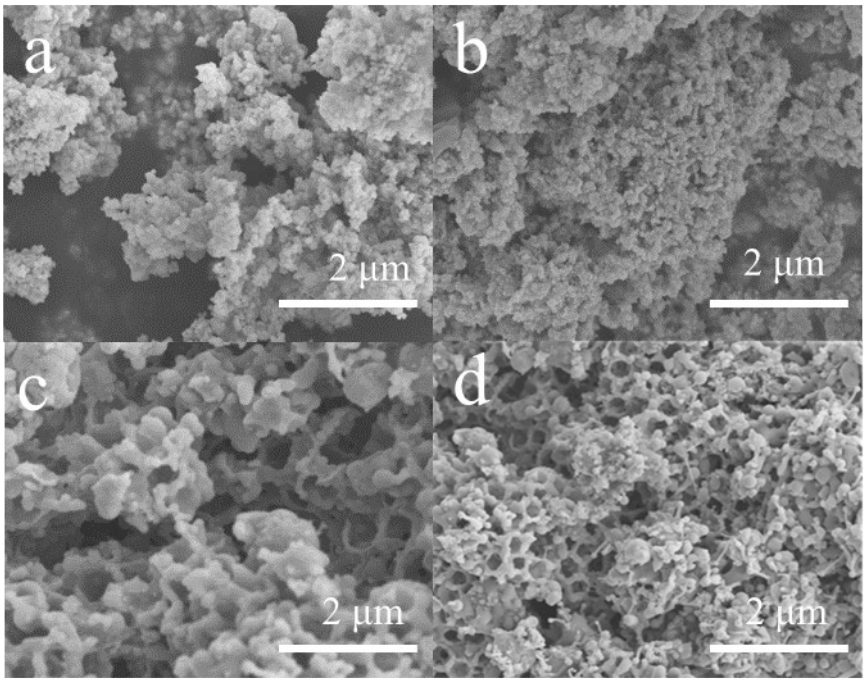

Fig. S1 SEM images of a) SnCu-1, b) SnCu -3, c) SnCuP/C-1, d) SnCuP/C-3.

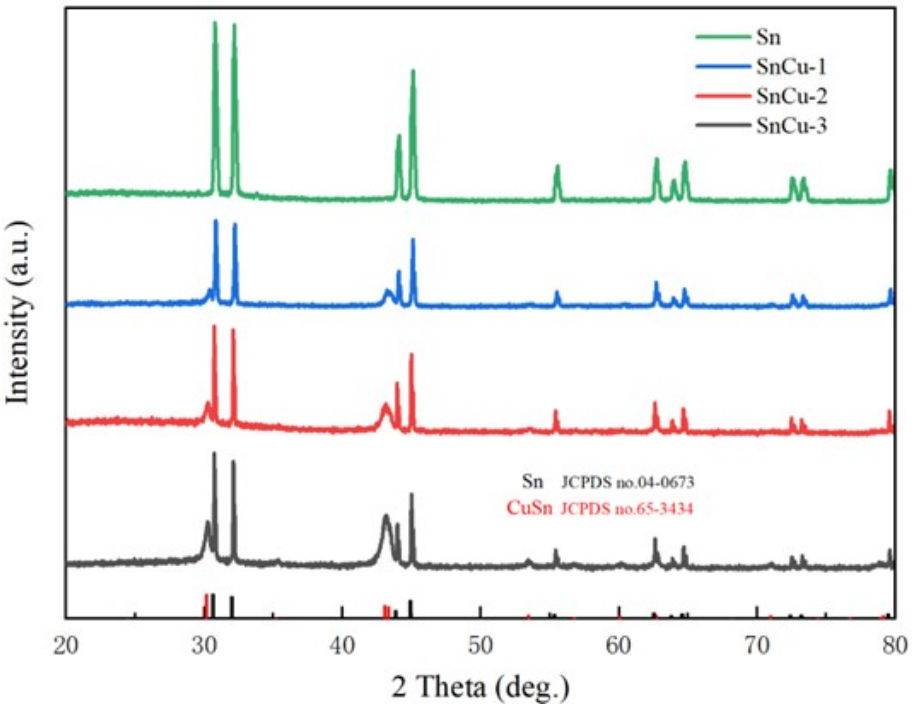

Fig. S2 XRD pattern of SnCu-X.

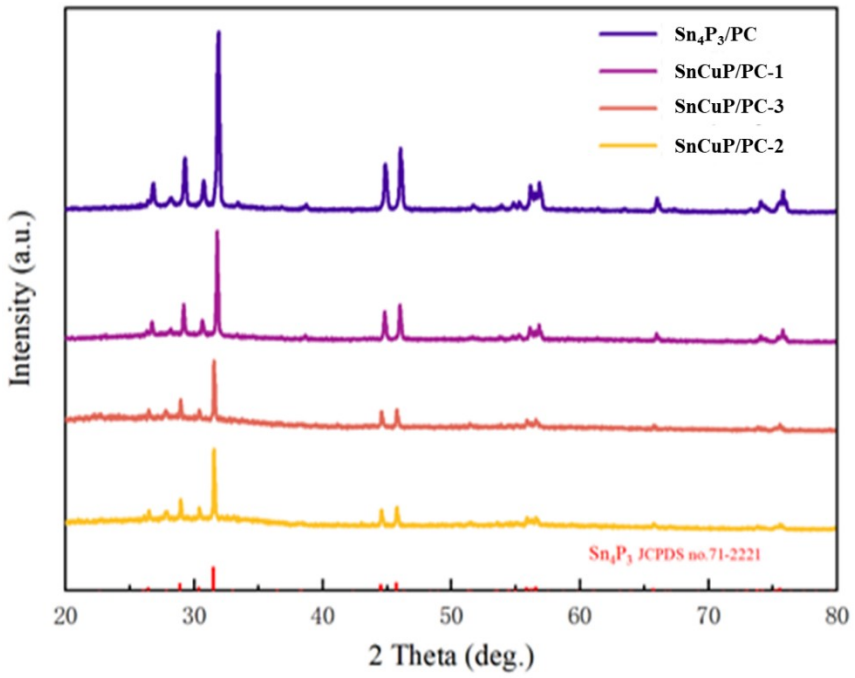

Fig. S3 XRD pattern of SnCuP/PC-X.

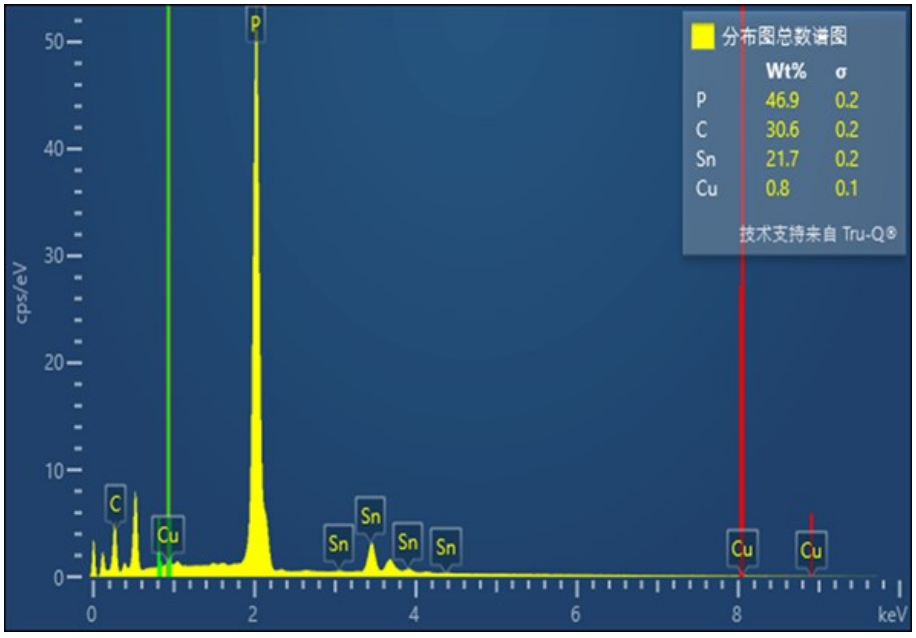

Fig. S4 EDX of the SnCuP/C-2 and the corresponding elemental content (the inset)

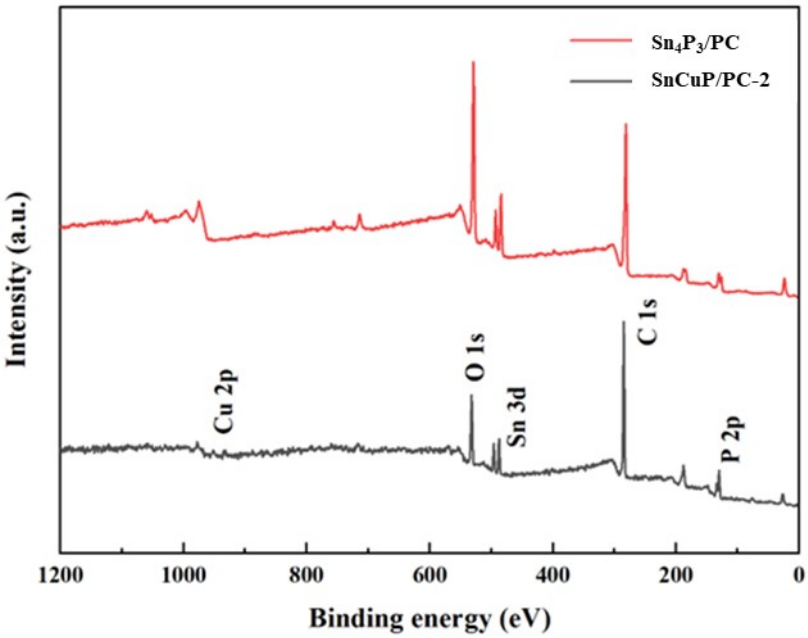

Fig. S5 XPS spectra of Sn_4P_3/PC and SnCuP/PC-2.

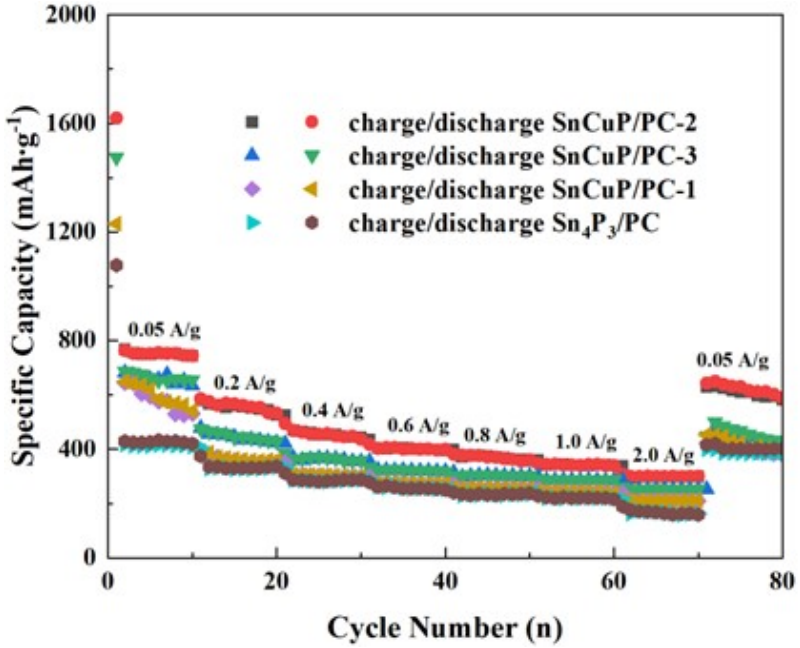

Fig. S6 Rate performance of SIBs with SnCuP/PC-X;

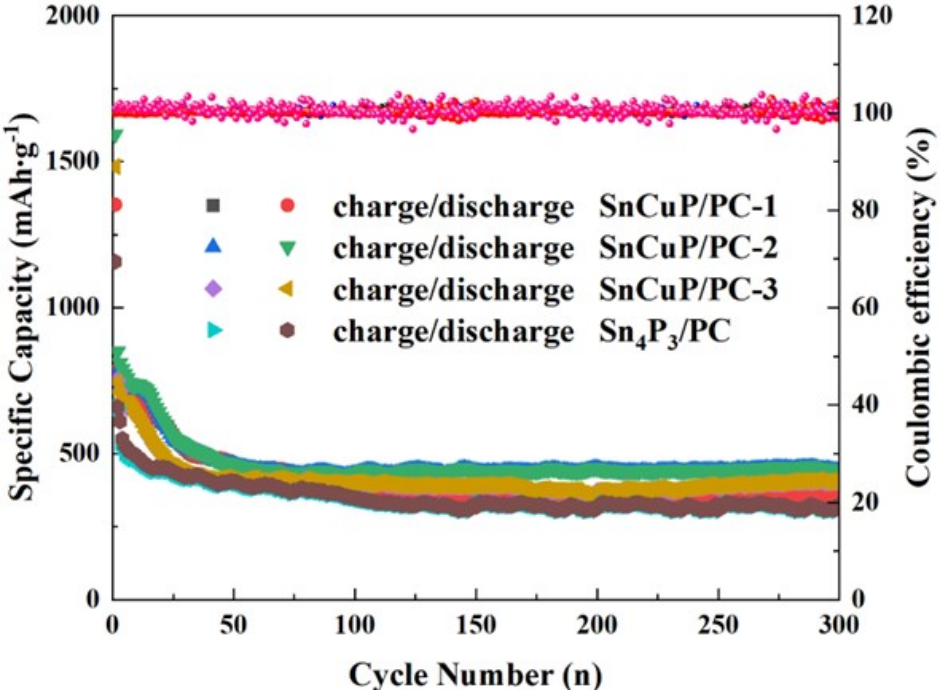

Fig. S7 Cycling performance of SIBs with SnCuP/PC-X at 0.2 A g^{-1}.

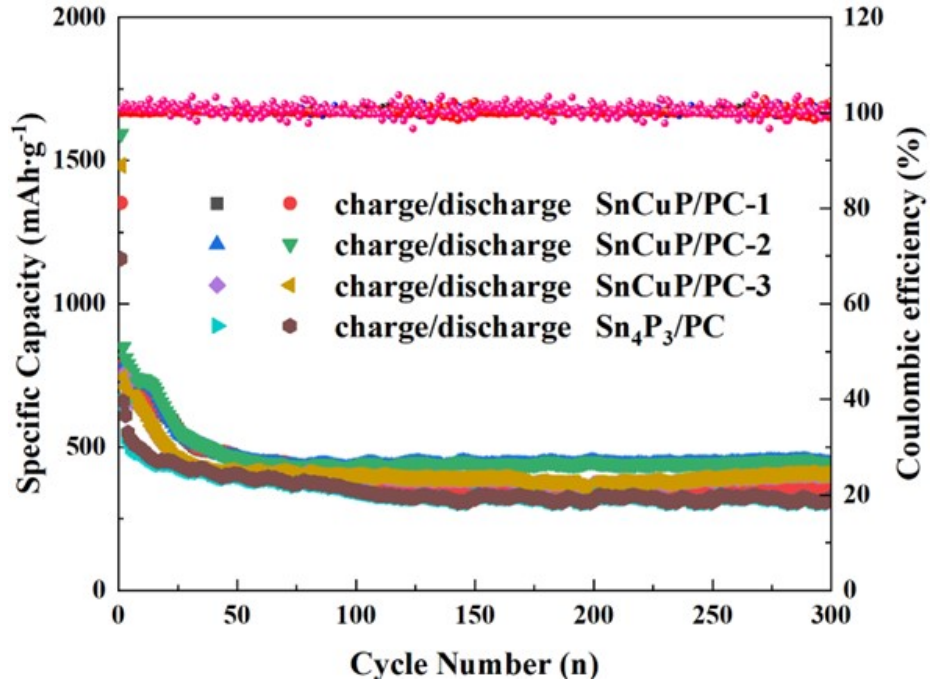

Fig. S8 Cycling performance of SIBs with SnCuP/PC-X at 1.0 A g^{-1}.

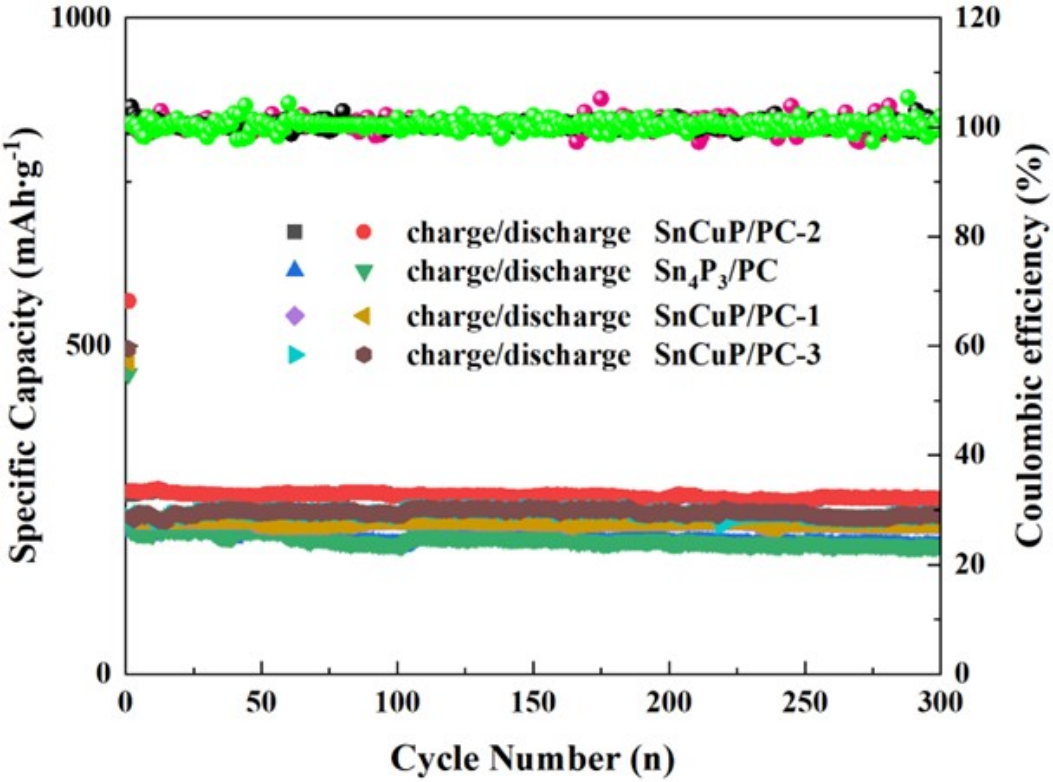

Fig. S9 Cycling performance of SIBs with SnCuP/PC-X at 2.0A g^{-1}.

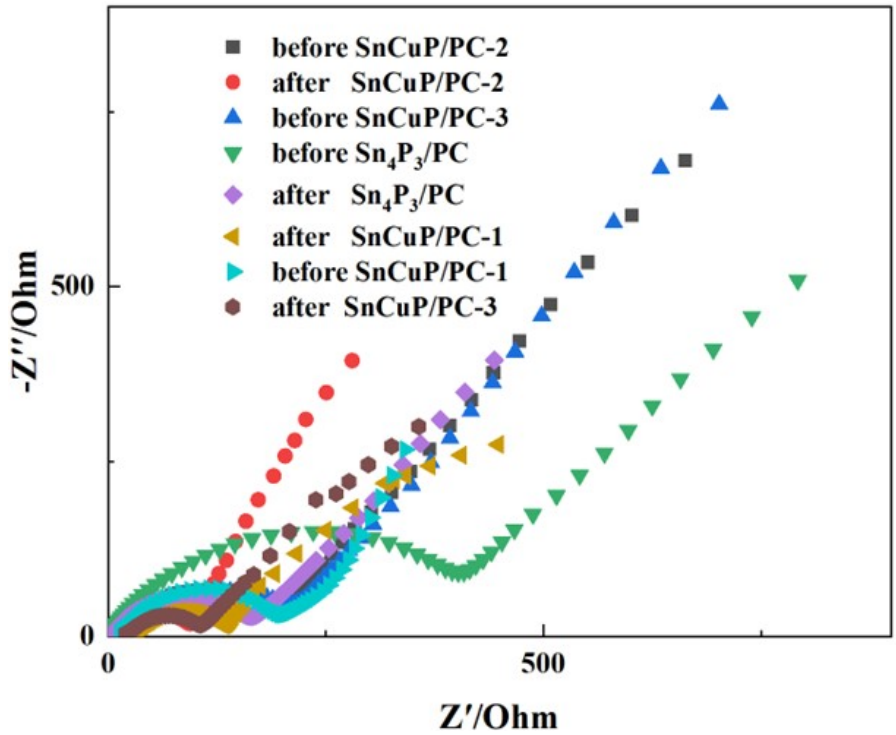

Fig. S10 Nyquist plots of the SIB with SnCuP/PC-X before and after 300 cycles.

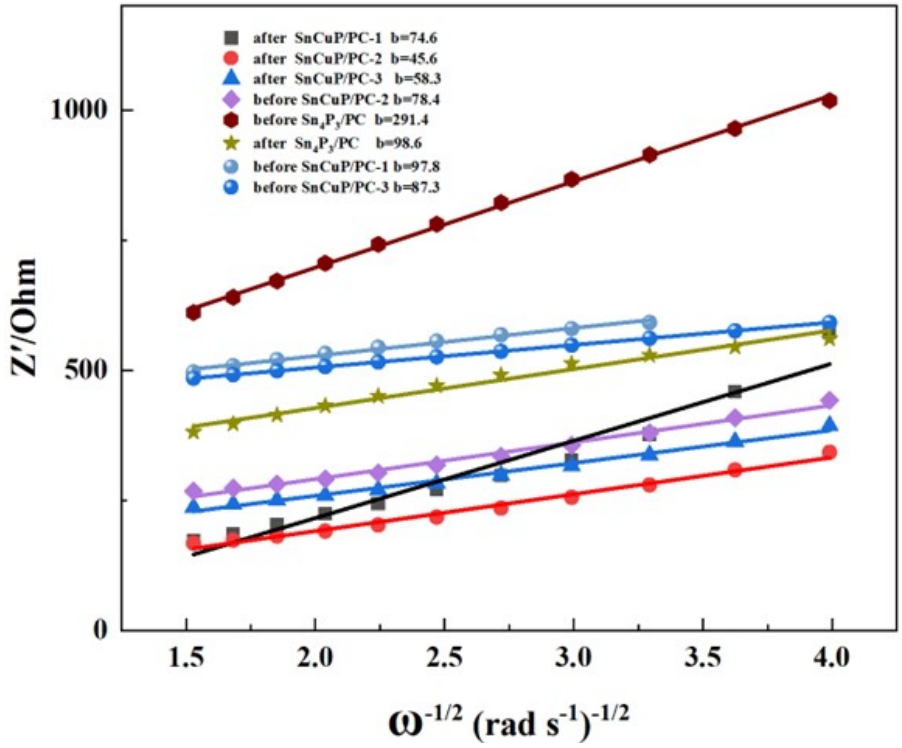

Fig. S11 The relationship between Z' and $\omega^{-1/2}$ of the SIB with SnCuP/PC-X in low frequency region.